25th ABCM International Congress of Mechanical Engineering
October 20-25, 2019, Uberlândia, MG, Brazil

COB-2019-0661
CHARACTERIZATION OF LEAN PREMIXED TURBULENT SWIRLING COMBUSTION REGIMES USING OH PLANAR LASER INDUCED FLUORESCENCE MEASUREMENTS

Gabriela Senra Pessanha Rios Nobrega
Letícia Carneiro Piton
Luís Fernando Figueira da Silva
Pontifícia Universidade Católica do Rio de Janeiro - Department of Mechanical Engineering
R. Marquês de São Vicente, 225 - 22451-900 - Gâvea, Rio de Janeiro, Brazil
gabi.senra@hotmail.com

Philippe Scouflaire
Nasser Darabiha
Laboratoire EM2C, CNRS, CentraleSupelec, Université Paris-Saclay - 3, Rue Joliot-Curie - 91192 Gif-sur-Yvette, France

Abstract. *Turbulent swirling combustion is often used for promoting stability in a wide range of flow conditions. Lean premixed combustion reduces NOx and soot emissions without reducing energetic efficiency, compared to classical non-premixed systems. This configuration is commonly applied to gas turbines and industrial burners. The present work is devoted to characterize lean premixed turbulent swirling combustion regimes in a laboratory burner with confinement. Five different combustion regimes have been observed and classified according to stability and structure of the flames. Planar laser induced fluorescence of OH radical has been used to characterize the topology of the flames. These PLIF-OH measurements allow to identify a reaction progress variable and, also, the corresponding variance. Combustion regimes diagrams are identified here as functions of the equivalence ratio and total volumetric flow rate of a CH_4/air mixture. The regimes obtained are shown to be controlled by the mixture equivalence ratio mostly.*

Keywords: *premixed turbulent combustion, swirling flow, flame stabilization*

1. INTRODUCTION

Premixed turbulent combustion with lean fuel/air mixtures is an alternative to reduce the emission of pollutant gases in industrial turbines and burners. These turbulent flames are often considered to be applied in confined configurations and in the presence of swirling fluid motion. Indeed, the influence of the swirling motion has been shown to exert a significant influence on the flame topologies, on the blow-off and flashback limits and on the acoustic stability properties (Candel *et al.*, 2014). Furthermore, turbulent swirling combustion is capable of improving flame stability those equipment combustion chambers and has thus been analyzed in several studies (Guiberti *et al.*, 2014; Jourdaine *et al.*, 2017). Huang and Yang (2009) have performed an extensive review of the coupling between the flow dynamics and the excitation of combustion instabilities, identifying the relevant mechanisms and associated controlling parameters. Candel *et al.* (2014) reviewed the state of the art of combustion in swirling flows, focusing on the influence of swirl number on the flow structure and on acoustic instabilities onset and control. Using a combination of an axial swirler and a bluff-body, Cavaliere *et al.* (2013) demonstrated that a Damköhler blow-off number could be expressed for different flames structures as a function of the combustor power.

Several studies have focused on the description of the different flame topologies that arise in premixed swirling combustors, on the associated flowfield structures and on the corresponding controlling parameters. Generally, an outer recirculation zone (ORZ) is located at the the vicinity of corners of the injection plane and adjacetn to combustion chamber walls (Taamallah *et al.*, 2015, 2017), whereas an internal recirculation zone (IRZ) has been shown to be formed near the burner center due to the flow expansion within the combustor and of the swirling motion influence. These recirculation zones have been demonstrated to decisively contribute to the flame stabilization. Modifications in fuel and air flow rates, reactant composition, injection temperature or operating pressure have been found to imply in changes of the swirling flame shapes (Guiberti *et al.*, 2014). These flames have been found to stabilize with either a “V” or an “M” shape at the vicinity of the mixture injector outlet. The V-shape flame has been shown to stabilizes at the vicinity of the inner shear layer (ISL), which is formed between the mixture jet entering combustion chamber and the IRZ. The M-flame is stabilized

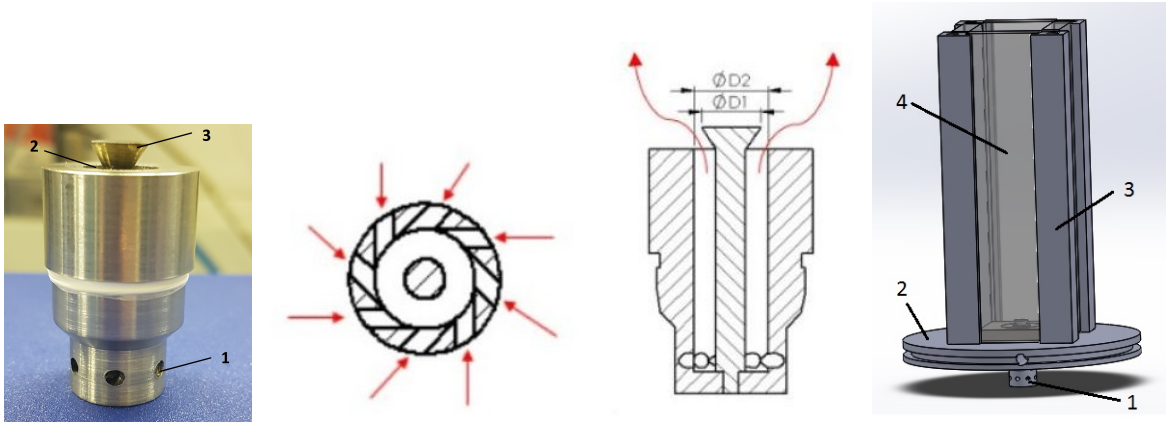

(a) Swirler: 1 - fuel/air mixture inlet orifices, 2 - flow outlet area, 3 - bluff-body.

(b) Swirler intlet area.

(c) Swirler oulet area.

(d) Combustion chamber: 1 - swirler, 2 - cooling base, 3 - confinement, 4 - quartz window.

Figure 1. Swirler and combustion chamber.

at the ISL, and features a tip toward the outer shear layer (OSL), which is found to occur between the ORZ and the fresh reactants flow. Concerning now the parameters controlling the flame shape change from V to M, Chterev *et al.* (2014) have shown that the dependency of the transition points on the flow velocity, fuel/air ratio and temperature when the flame is stabilized in the inner and outer shear layers. Besides, when the flame attaches/detaches from the OSL the flow field exhibit changes, particularly at the ORZ. Mallens *et al.* (1997) concluded that the transition from M to V shape flame starts with the detachment of the M shape flame at the outer burner wall leading to a V shape flame, but that this transition does not happen suddenly.

The present work follows the initial characterization of different lean premixed combustion regimes (Figueira da Silva *et al.*, 2017; Piton *et al.*, 2018; Nobrega *et al.*, 2019) by analyzing the flame topologies and studying flame/wall interaction in a bluff-body configuration similar to the one developed in Cavaliere *et al.* (2013). This analysis is performed by utilizing planar laser induced fluorescence (PLIF) of the OH radical in order to evidence the flame structure, as well as the flame surface density. The studied burner has been developed in a partnership between PUC-Rio and EM2C/CNRS laboratory at CentraleSupelec, and is called BEST Flame (Bioethanol Swirl Turbulent). The final objective of this partnership is to study and analyze the developed burner stability when using ethanol/air lean pre-vaporized mixtures.

The paper proceeds by first presenting the studied swirlers and the measurement methodology. Then, the results obtained using a methane/air mixture are discussed. The structure of the flames is evidenced by the use OH PLIF, and the combustion regimes are mapped for one type of swirler as a function of mixture flow rate and equivalence ratio. Finally, conclusions and perspectives of future works are given.

2. EXPERIMENTAL METHODOLOGY

The test bench used in this work has been designed to enable flame imaging, control the flow of the fuel/air mixture and to maintain the laser plane perpendicular to the intensified camera. A scheme of the experimental setup may be found elsewhere (Piton *et al.*, 2018). The experimental setup consists of the burner, the combustion chamber, a methane and air flowmeter, a flow controller, an intensified CCD camera, a dye laser pumped by an Nd:YAG laser. For the methane flow, a Bronkhorst flow controller (F-201AC series) has been used, with a full scale of 0.5 Nm^3/h and 0.1% uncertainty. Also for the air flow a flow controller of the brand Bronkhorst (series F-202AV) has been used, with full scale 5 Nm^3/h and 0.1% uncertainty. The flow control is performed through an electronic device that adjusts the percentage of the flow rate. In this work, the total volumetric flow rate of the mixture varies from 397.2 cm^3/s to 1448.1 cm^3/s.

2.1 Swirlers and Combustion Chamber

Figure 1(a) illustrates an example of one of the studied radial swirlers. Figures 1(b) and 1(c) allow to observe the inlet and outlet areas of the through which the fuel/air mixture flows before issuing to the combustion chamber. The methane/air mixture first flows through the orifices at the bottom of the swirler, which are inclined relative to the main axis. As a consequence, a swirling motion is imparted to the mixture, which is fed tangentially to the swirling chamber. Inside the swirling chamber there is a 4 mm central cylinder with an inverted cone which upper base has a diameter of 8 mm. This inverted cone acts as a bluff-body, allowing to stabilize the flame. Different heights central cylinders have been developed to analyze the effect of this parameter on combustion stability and flame structure (Nobrega *et al.*, 2019). In this work, a six orifices swirler with central cylinder flushed to the swirler surface has been used. This swirler is dubbed

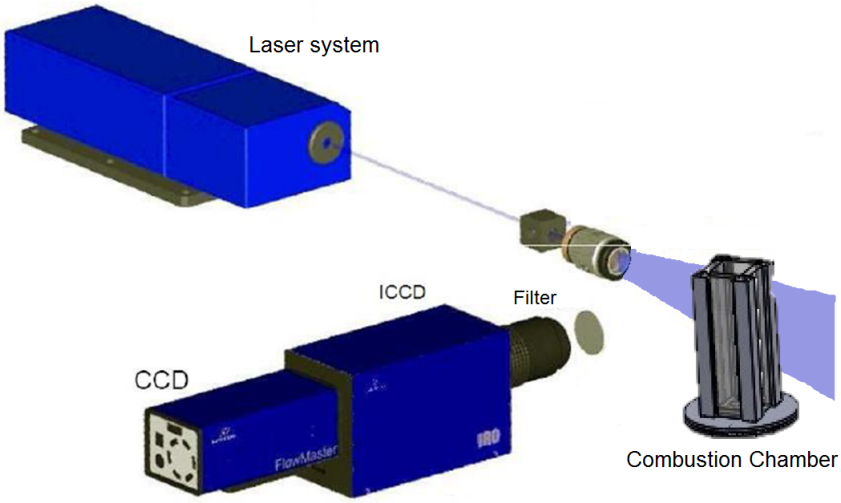

Figure 2. Schematic representation of the experimental setup.

SW06I and its swirl number is $S = 0.4$. Figure 1(d) shows the developed combustion chamber, whchi is square and each side has a width of 40 mm.

The methane/air mixture is introduced via the swirler, represented in this figure by the number 1. The combustion chamber consists of four vertical quartz windows, with 10 mm thickness that are transparent to UV radiation, and a water-cooled base, since it may be in contact with high temperature gases. The quartz allows the visualization of the combustion region, and is resistant to high temperatures. An insulation blanket is used to prevent the quartz and supporting structure to merge and to reduce the risk of thermal expansion cracking the of window.

2.2 Planar laser induced fluorescence

Laser-induced fluorescence (LIF) is the spontaneous emission of radiation by atoms or molecules that have been excited by laser radiation (Kohse-Höinghaus and Jeffries, 1989). It is often applied in combustion processes to measure species concentration and to obtain temperature. In the case of the PLIF technique, planar laser-induced fluorescence, laser radiation is used in the form of a thin plane, making it possible to obtain the two or three dimensional mapping of species present in the flame.

A scheme of the optic diagnostics setup is given in Fig. 2. A dye laser system and an intensified CCD camera (ICCD) have been used in the tests. The laser sheet is perpendicularly aligned with the camera, so as to avoid geometric distortion of the image plane, and passes through the center of the combustion chamber.

In the present work a Nd:YAG laser (Quantel, Brilliant B) has been used at 355 nm, third harmonic, for the purposes of pumping a dye laser. It has pulse duration of 7 ns and it has been operated at a power ranging from 1.2 W to 1.57 W, with a 10 Hz repetition rate. The dye laser used is the Sirah, model CSTR-G-3000. This equipment allows the tuning of a large range of wavelengths, in which the chemical species are excited. Here, ethanol-diluted Coumarin-153 dye has been used to study the OH radical at an excitation wavelength of 287.56 nm. This wavelength excites an electronic transition of OH radical, $Q_1(8)$, from the rotational state ($\nu' = 0$) and vibrational state ($\nu'' = 1$), of the system A-X (1, 1) and (0, 0) of the $j = 8$ transition (Caetano and Figueira da Silva, 2015).

An externally-intensified camera is used to observe the OH fluorescence signal. LaVision IRO (Intensified relay-optics) coupled to an Imager Intense CCD camera of the same brand has been used. A 310 nm band-pass filter has been used in order to observe the OH radical. The ICCD is controlled by the computer during image acquisition, adjusting the desired data acquisition time. More detailed information of the experimental setup may be found in previous works (Nobrega *et al.*, 2019).

For the purpose of analysis, each instantaneous OH-PLIF image is binarized. The binarization procedure results in the value 1, when the PLIF-OH signal lies above a threshold immediately superior to the background noise, and 0 otherwise. Therefore, since OH is found both at the flame surface and at the burned gases, c may be interpreted as a progress variable. This progress variable is supposed to represent the temperature of the unburned (c=0) and burned (c=1) gases.

3. RESULTS AND DISCUSSION

3.1 Flame topology identification

Planar laser induced fluorescence has been thus applied to characterize the flame topology. The experimental procedure consists in starting from the highest methane equivalence ratio and mixture flow rate. By decreasing the fuel concentration in the mixture, it is possible to observe different combustion regimes, until the flame extinguishes, i.e., the blow-off limit is attained.

Figure 3 shows the results that have been obtained using a swirler with six orifices and bluff-body having the same height as the exit surface of the swirler. In this figure each row represents a different combustion regime. Indeed, the stable regime I is the one where the flame presents the tornado shape and is lifted from the swirler base. The images of this regime were obtained at equivalence ratio of $\phi = 0.57$ and the maximum operational flow rate, $\dot{\forall} = 1430$ cm^3/s. This figure allows to observe that the flame does not interact with the combustion chamber walls. Regime II corresponds to an unstable regime where the flame flickers and is a transition situation between regimes I and III. The OH-PLIF results of this regime have been obtained at equivalence ratio and flow rate equal to $\phi = 0.62$ and $\dot{\forall} = 1430$ cm^3/s, respectively. In regime III, the flame has a V-shape and is stable. For this regime, all images have been obtained at $\phi = 0.70$ and $\dot{\forall} = 1440$ cm^3/s. In this regime the flame is anchored to the swirler surface. Stable regime IV is that of a M-shape flame, a regime where there are combustion products in an outer recirculation zone and strong interaction with the flame confinement. The images have been obtained at $\phi = 0.73$ and $\dot{\forall} = 1450$ cm^3/s.

Furthermore, in Fig. 3 each column shows a different property. The first one, column A, represents a binarized instantaneous image of the OH radical in each regime, $c(x, y, t)$. Each of the studied flame regimes correspond to a rather different instantaneous picture. The flame in regime I is lifted from the burner surface and it is corrugated. The instantaneous image shows that the flame in regime II is also corrugated, presenting pockets of OH radical. For the regime III, the instantaneous picture shows the V shape flame and for regime IV, it indicates the presence of OH radical in the outer recirculation zone.

Column B shows the ensemble average of 4,000 binarized instantaneous images, $\bar{c}(x, y)$, which gives the probability of observing the OH radical in the combustion chamber. This column indicates that flame in regime I is detached from the swirler base and is predominantly located above the center of the combustion chamber. This column also reveals that regime II features two maxima, showing that the flame shape changes between V shape flame and the lifted flame. For regime III, the average of the binarized images evidences that there is no OH radical in the outer recirculation zone, thus there is no probability of observing burnt gases in this area. Column B indicates, for regime IV, the presence of burnt gases in the corner of the combustion chamber base, at the outer recirculation zone. Classically, following the Bray-Moss-Libby assumptions, the instantaneous adiabatic flame front thickness is supposed to be small when compared to the turbulence length scales.Thus, for lean turbulent premixed combustion, temperature and fuel mass fraction could be described by a progress variable c, $0 \leq c \leq 1$, and the PDF of c is given by a double Dirac function, $P(c) = (1 - \bar{c})\delta(c) + \bar{c}\delta(1 - c)$. As consequence the variance of c, is $\sigma^2 = \bar{c}(1 - \bar{c})$. Note that σ^2 is also proportional to a flame surface density and thus could be used for the purpose of comparisons with turbulent combustion models (Poinsot and Veynante, 2005).

Column C shows the computed variance $\sigma^2(x, y)$, whereas column D represents $\bar{c}(x, y) \times [1 - \bar{c}(x, y)]$. For regime I, column C shows that the flame oscillates around the lifted position. Column C for the regime II represents a situation where the flame flickers, alternatively assuming the V shape or the lifted format. The variance shown in this column allows to observe that the flame front in regime III is adjacent the wall of the confinement. In regime IV, fluctuations arise at the outer recirculation zone, indicating that in the middle of the combustion chamber there are only burnt gases and that the flame front is located near the outer recirculation zone.

Figure 3 allows to compare the measured values of σ^2 and $\bar{c}(1 - \bar{c})$, given in columns C and D, respectively. A first analysis indicates that, due to the strong flame/wall interaction, the measured flames could not be described by a single scalar, i.e., the process variable. Indeed, the strong gradients of c at the wall vicinity in regimes III and IV indicate that the additional equations should be used to describe these flame/wall interactions.

Figure 4 shows the OH-PLIF signal at different heights for each combustion regime, represented in each row and for each property, represented in the columns. The different heights have been chosen to show the properties along the combustion chamber: the bottom, near the swirler exit (y=10 mm); the middle (y=30 mm) and the top (y=50 mm). Column B represents the average of the 4,000 binarized images. The vertical scale ranges from zero to one. Column C shows the computed variance $\sigma^2(x, y)$ and column D indicates $\bar{c}(x, y) \times [1 - \bar{c}(x, y)]$. The maximum value of σ^2 marks the position of the flame front.

Analyzing each height for the regime I, it is possible to confirm that the flame is not attached to the swirler. At $y = 10$ mm and $y = 30$ mm the average of the images and variance is small, indicating that the flame front does not lie in that position. At $y = 50$ mm the variance has considerable value, around 0.2, showing that the flame front is located between $-10 \leq x \leq 10$ mm and is lifted from the bluff-body.

Column C indicates that the flame front in regime II is distributed along the combustion chamber, i.e. $\sigma^2 \approx 0.25$ almost everywhere, but the flame does not interact strongly with the wall.

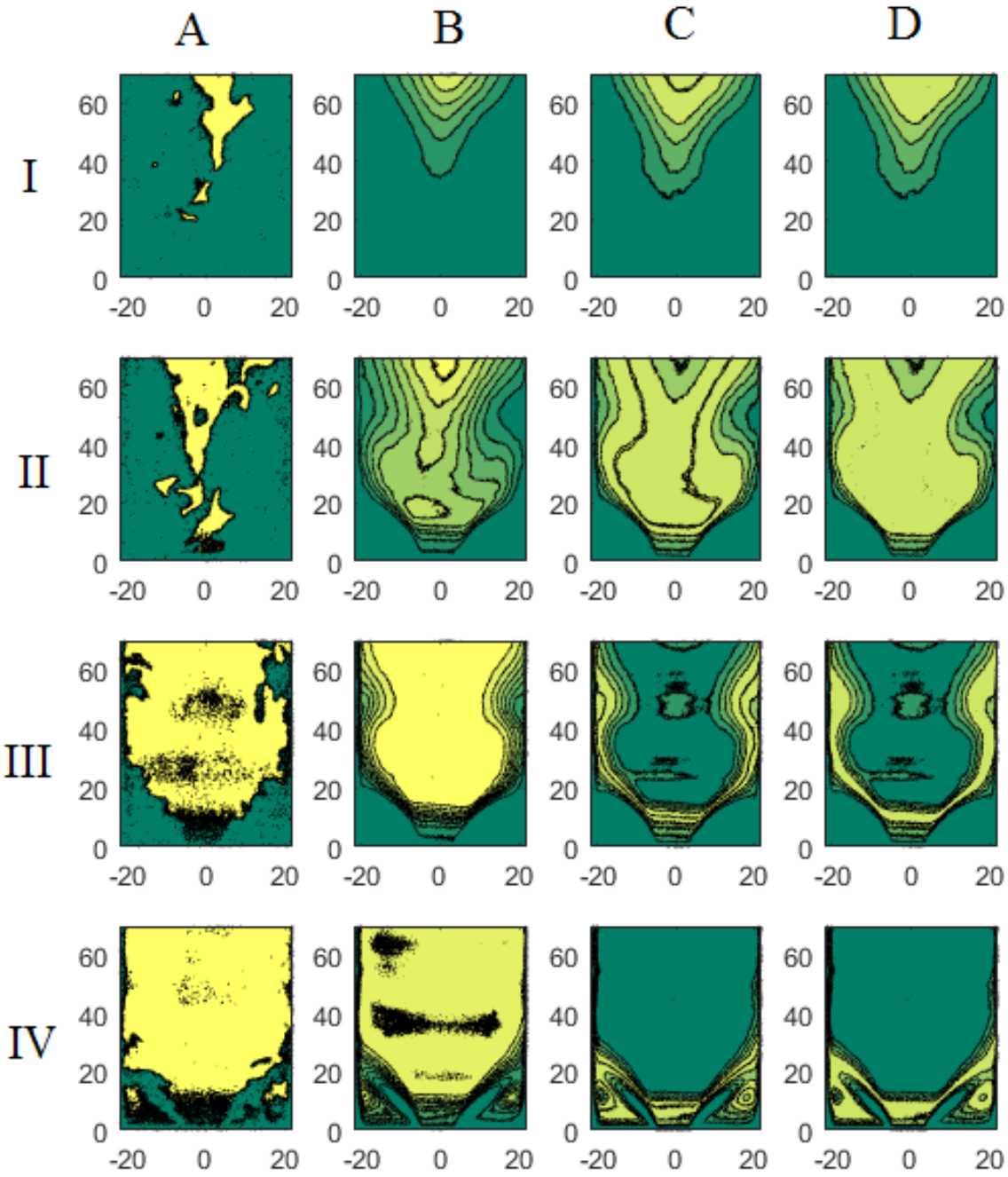

Figure 3. Binarized PLIF-OH images. The Roman numerals correspond to the flame regimes I: lifted tornado flame; II: unstable regime; III: V-shape flame; IV: M-shape flame, and the capital letters denote: A: instantaneous field $c(x, y)$; B: ensemble average field $\bar{c}(x, y)$; C: variance $\sigma^2(x, y)$ and D: $\bar{c}(x, y) \times [1 - \bar{c}(x, y)]$.

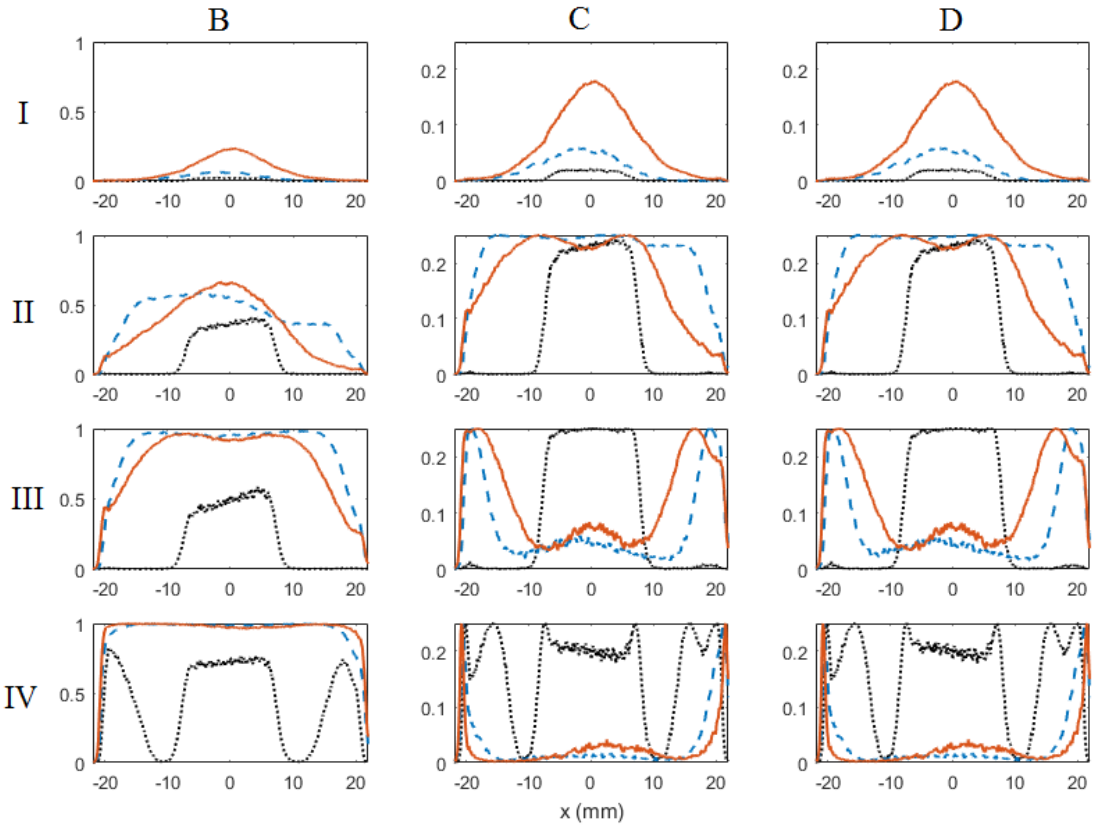

Figure 4. PLIF-OH signals at different heights: $y = 10\,(\cdots)$, 30 (- - -) and 50 mm (—). The Roman numerals correspond to the flame regimes I: lifted tornado flame; II: unstable regime; III: V-shape flame; IV: M-shape flame, and the capital letters denote: B: ensemble average field $\bar{c}(x, y)$; C: variance $\sigma^2(x, y)$ and D: $\bar{c}(x, y) \times [1 - \bar{c}(x, y)]$.

For regime III, column B shows that for $y = 10$ mm the position of the flame front is concentrated at the vicinity the swirler exit and the probability of having OH radical near the confinement wall is zero, whereas for $y = 30$ mm and $y = 50$ mm it is mostly observed burnt gases. The variance, column C, for this regime shows that at $y = 10$ the flame front lies between $-10 \leq x \leq 10$ mm and for $y = 20$ and $y = 50$ mm the flame front stands closer to the combustion chamber wall, where σ^2 is maximum.

In regime IV, column B shows the outer recirculation zone flame at $y = 10$ mm and also shows that at $y = 30$ and $y = 50$ mm that only burnt gases are found. For this regime, column C evidences that at $y = 10$ mm that are two flame fronts, an inner, at $-10 \leq x \leq 10$ mm, and an outer, at $10 \leq x \leq 20$ mm flame front due to the outer recirculation zone. For $y = 20$ mm and $y = 50$ mm the flame front is adjacent to the confinement wall.

3.2 Combustion regimes diagram

The observed combustion regimes have been classified according to the flow structures observed visually and acoustically. The mixture volume flow rate and the equivalence ratio have been chosen to construct the combustion regimes diagrams shown in Fig. 5. The diagram presented has been obtained for swirler SW06I, corresponding to bluff-body flushed to the swirler surface. For this swirler the calculated geometric swirl number is $S = 0.4$. Each symbol represents a boundary between the regimes. The highest equivalence ratio leads to the M-shape flame in regime IV. Upon decreasing the equivalence ratio, the unstable regime IVf is observed, where the flame flickers and the OH radical is present at the outer recirculation zone. A further equivalence ratio decrease, stable regime III is reached, in which the flame presents a V-shape. Another decrease in the fuel concentration in the mixture leads to a second unstable flickering regime, II. For a lower equivalence ratio, a stable regime I is achieved, where the flame exhibits a spiral shape. Decreasing again the equivalence ratio, the combustor lean blow-off occurs. The combustion regimes diagram shows that the boundary between regimes IV and IVf corresponds to a maximum equivalence ratio of 0.87 and a minimum blow-off at 0.4. Stable regime I occurs in a range of equivalence ratio from 0.4 to 0.6 and regime III occurs from 0.62 to 0.7. The stability of regime I happens at lower equivalence and its stability is easier to be maintained than regime III, improving the operation conditions. This regime diagram figure also allows to observe that the mixture flow rate influence on the observed regime

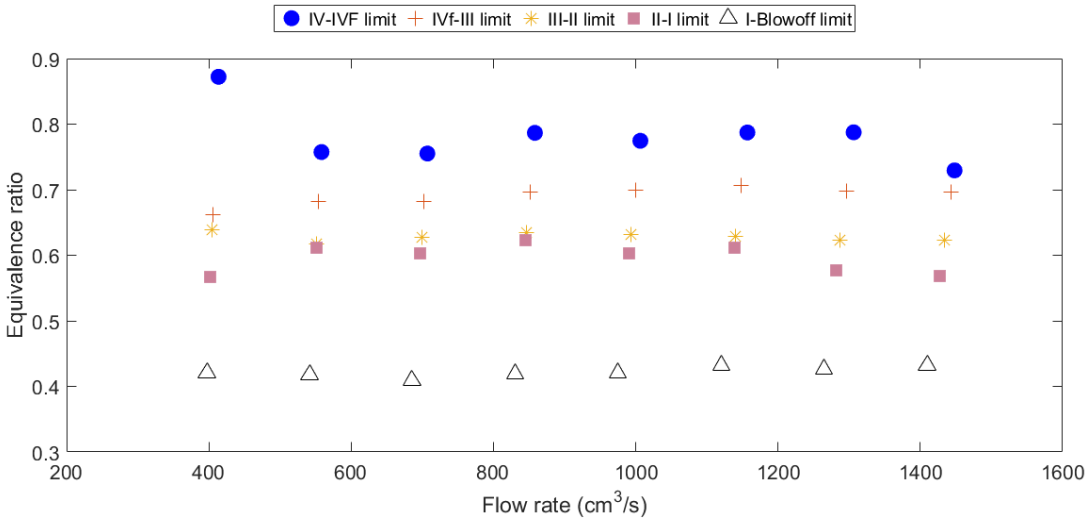

Figure 5. SW06I: Combustion regime diagram, $S = 0.4$.

is nearly imperceptible, at least for the considered operational regime.

4. CONCLUSIONS

The planar laser-induced fluorescence (PLIF) of the OH radical technique was performed to analyze the flame topology for different combustion regimes. The instantaneous binarized images were interpreted as a progress variable since the OH radical is found at the flame surface and at the burned gases. The computed variance allowed to observe the position of the flame front and compare the average flame thickness along the combustion chamber.

The combustion regimes were mapped into a diagram as function of mixture flow rate and equivalence ratio, evidencing stable and unstable regimes.

In order to futher characterize the flow field strutures, future work will measure the flow velocity using the particle image velocimetry technique. Also, combustion regimes will be investigated for prevaporized ethanol/air mixtures and the structure of the flames will be analyzed using the planar laser induced fluorescence of the radical OH technique.

5. ACKNOWLEDGEMENTS

This work was supported by PUC-Rio and Laboratoire EM2C CNRS, CentraleSupelec (France). L.F. Figueira da Silva was on leave from the Institut Prime (CNRS, France), L.C. Piton and G.S. Nobrega had scholarships from CNPq (Brazil). The authors gratefully acknowledge the support for the present research provided by Conselho Nacional de Desenvolvimento Científico e Tecnológico, CNPq, under the Research Grants No. 306069/2015-6 and 304444/2018-9. Support from Laboratoire International Associé Energie et Environement is also gratefully acknowledged.

6. REFERENCES

Caetano, N.C. and Figueira da Silva, L.F., 2015. "A comparative experimental study of turbulent non premixed flames stabilized by a bluff-body burner". *Experimental Thermal and Fluid Science*, Vol. 63, pp. 20–33.

Candel, S., Durox, D., Schuller, T., Bourgouin, J. and Moeck, J., 2014. "Dynamics of swirling flames". *Annual Review of Fluid Mechanics*, Vol. 46, pp. 147–173.

Cavaliere, D., Kariuki, J. and Mastorakos, E., 2013. "A comparison of the blow-off behaviour of swirl-stabilized premixed, non-premixed and spray flames". *Flow, Turbulence and Combustion*, Vol. 91, pp. 349–372.

Chterev, I., Foley, C.W., Foti, D., Kostka, S., Caswell, A.W., Jiang, N., Lynch, A., Noble, D.R., Menon, S., Seitzman, J.M. and Lieuwen, T.C., 2014. "Flame and flow topologies in an annular swirling flow". *Combustion Science and Technology*, Vol. 186, pp. 1041–1074.

Figueira da Silva, L.F., Mergulhão, C.S., Piton, L.C., Scouflaire, P. and Darabiha, N., 2017. "Experimental study of a lean premixed turbulent swirling flame stabilization". In *24th ABCM International Congress of Mechanical Engineering*. Curitiba, Brazil, pp. 766–773.

Guiberti, T.F., Durox, D., Zimmer, L. and Schuller, T., 2014. "Analysis of topology transitions of swirl flames interacting with the combustor side wall". *Combustion and Flame*, Vol. 162, No. 11, pp. 4342–4357.

Huang, Y. and Yang, V., 2009. "Dynamics and stability of lean-premixed swirl-stabilized combustion". *Progress in*

Energy and Combustion Science, Vol. 35, pp. 293–364.

Jourdaine, P., Mirat, C., Caudal, J., Lo, A. and Schuller, T., 2017. "A comparison between the stabilization of premixed swirling CO_2- diluted methane oxy-flames and methane/air flames". *Fuel*, Vol. 201, pp. 156–164.

Kohse-Höinghaus, K. and Jeffries, J.B., 1989. *Applied combustion diagnostics*. CRC Press, New York, N.Y., 1st edition.

Mallens, R.M.M., Loijenga, B.O., De Goey, L.P.H. and Sonnemansb, P.J.M., 1997. "Numerical and experimental study of lean m-and v-shaped flames". *Combustion Science and Technology*, Vol. 122, pp. 331–344.

Nobrega, G.S., Piton, L.C., Figueira da Silva, L.F., Scouflaire, P. and Darabiha, N., 2019. "Experimental study of the effect of the swirl number on premixed combustion regimes and flame topologies". In *11th Mediterranean Combustion Symposium (MCS 2019)*. Tenerife, Spain.

Piton, L.C., Nobrega, G.S., Figueira da Silva, L.F., Scouflaire, P. and Darabiha, N., 2018. "Experimental study of the influence of the swirl number on lean premixed combustion regimes". In *17th Brazilian Congress of Thermal Sciences and Engineering*. Águas de Lindóia, SP, Brazil, pp. 1–8.

Poinsot, T. and Veynante, D., 2005. *Theoretical and Numerical Combustion*. R. T. Edwards Inc., Philadelphia, PA 19118 USA, 2nd edition.

Taamallah, S., Chakroun, N.W., Watanabe, H., Shanbhogue, S.J. and Ghoniem, A.F., 2017. "On the characteristic flow and flame times for scaling oxy and air flame stabilization modes in premixed swirl combustion". *Proceedings of the Combustion Institute*, Vol. 36, No. 3, pp. 3799–3807.

Taamallah, S., Labry, Z.A., Shanbhogue, S.J. and Ghoniem, A.F., 2015. "Thermo-acoustic instabilities in lean premixed swirl-stabilized combustion and their link to acoustically coupled and decoupled flame macrostructures". *Proceedings of the Combustion Institute*, Vol. 35, pp. 3273–3282.